Journal of Hydrology 519 (2014) 656–669

Contents lists available at ScienceDirect

Journal of Hydrology

journal homepage: www.elsevier.com/locate/jhydrol

Vadose zone lag time and potential 21st century climate change effects on spatially distributed groundwater recharge in the semi-arid Nebraska Sand Hills

N.R. Rossman [a,*], V.A. Zlotnik [a], C.M. Rowe [a], J. Szilagyi [b,c]

[a] Department of Earth and Atmospheric Sciences, University of Nebraska-Lincoln, Lincoln, NE 68588, USA
[b] School of Natural Resources, University of Nebraska-Lincoln, Lincoln, NE 68583, USA
[c] Department of Hydraulic and Water Resources Engineering, Budapest University of Technology and Economics, Műegyetem Rakpart 1-3, H-1111 Budapest, Hungary

ARTICLE INFO

Article history:
Received 27 March 2014
Received in revised form 9 July 2014
Accepted 28 July 2014
Available online 7 August 2014
This manuscript was handled by Corrado Corradini, Editor-in-Chief, with the assistance of Rao S. Govindaraju, Associate Editor

Keywords:
Groundwater recharge
Climate change
Vadose zone
Lag time
Groundwater modeling
Nebraska Sand Hills

SUMMARY

Deep drainage of water below plant root zones (potential groundwater recharge) will become groundwater recharge (*GR*) after a delay (or lag time) in which soil moisture traverses the vadose zone before reaching the water table. Depending on the thickness of the vadose zone, the magnitude of deep drainage, and soil hydraulic properties, lag times will vary broadly, exceeding decades to centuries in semi-arid and arid environments. Yet, studies of future climate change impacts to *GR* have typically avoided focusing on impacts beyond 100 years and often neglect to consider lag effects caused by the vadose zone. We investigate the effects of vadose zone lag time and potential 21st century climate change on the spatial distribution and timing of *GR* throughout the semi-arid Nebraska Sand Hills (NSH) region (~50,000 km^2). We propose a simple and rapid quantitative approach for assessment of the groundwater system response time to changes in climate. Understanding of such effects is needed for groundwater modeling, analysis of climate change impacts on groundwater, and the effective management and sustainability of future water resources. Lag time estimates are made using the pressure-based vertical velocity of soil moisture changes, equivalent to a kinematic wave approximation of Richards' equation. The underlying assumptions (unit hydraulic gradient and relatively slow changes in climate) are supported by observations in the High Plains aquifer region, encompassing the NSH. The analysis relies on four sources of input data, including: Spatially distributed high resolution (1.1-km) *GR* rates (as the difference in 2000–2009 mean precipitation and evapotranspiration—estimated using a novel MODIS-based approach); thickness of the vadose zone—based on 30-m digital elevation models of the land surface and water table elevations; statistically downscaled estimates of future (2010–2099) potential *GR* rates from two hydroclimate model projections (WRCP CMIP3) with opposing *GR* trends; and estimates of hydraulic conductivity and vertical velocity of the vadose zone pressure changes using the van Genuchten–Mualem equation. We found that vadose zone lag times (with a mean *GR* rate of 78 mm/yr for 2000–2009) have an estimated spatial mean of 5.28 yrs (vertical velocity of 5.68 m/yr). End-of-century lag times (with mean potential *GR* rates of 128 and 61 mm/yr for 2090–2099) have estimated spatial means of 3.78 and 6.55 yrs (vertical velocities of 8.13 and 4.69 m/yr) for wet and dry scenarios, respectively. Findings suggest that the highly conductive materials (primarily sand deposits) and high potential *GR* rates in the NSH lead to relatively quick drainage of vadose zone water on the order of several years (less than a decade) for the entire 21st century. However, considerable spatial variations of lag times exist due to gradients in potential *GR* rates and the highly variable vadose zone thickness in the NSH.

1. Introduction

Climate-related variables such as the spatial distribution and intensity of precipitation (*P*) and evapotranspiration (*ET*) control soil water content in the vadose zone, the region between the land surface and saturated zone through which groundwater recharge (*GR*) can occur (Green et al., 2011). Groundwater systems in semi-arid and arid environments are especially sensitive to climate change because of the strong dependence of *ET* rates on temperature, and shifts in the precipitation regime affecting *GR* (Toews and Allen, 2009). Long-term changes in climate and land use have

* Corresponding author. Tel.: +1 402 472 2663; fax: +1 402 472 4917.
E-mail addresses: nrossman@huskers.unl.edu (N.R. Rossman), vzlotnik1@unl.edu (V.A. Zlotnik), crowe1@unl.edu (C.M. Rowe), jszilagyi1@unl.edu (J. Szilagyi).

http://dx.doi.org/10.1016/j.jhydrol.2014.07.057
0022-1694/

substantially affected *GR* rates in many regions of the world (Scanlon et al., 2006). While impacts to *GR* caused by land use changes are generally well understood (e.g., Cook et al., 2003; Scanlon et al., 2007), those caused by future climate change remain less certain. Thus, interest in this topic has increased greatly over recent years (e.g., Crosbie et al., 2013; Ferguson and Maxwell, 2012; Green et al., 2011; Gurdak et al., 2007).

Among the various hydrologic cycle components, *GR* is the leading variable determining groundwater resources availability and sustainability in semi-arid and arid environments (Crosbie et al., 2013; Szilagyi et al., 2011b). Of practical importance to groundwater modeling and water resource management are the effects of projected changes in potential groundwater recharge (GR_p) rates (deep drainage beneath the root zone) on multi-decadal to century time scales, because regions with deep water tables and/or experiencing low GR_p rates with fine-textured soils can have vadose zone lag times that exceed a century (McMahon et al., 2006; Scanlon et al., 2010). Thus, climate changes occurring within the 21st century (the period for which climate change projections are commonly made) may not affect groundwater resources within the same time frame, and steady actual groundwater recharge (GR_a) rates (flux across the water table) will remain unchanged.

Even when estimates of GR_p rates have a sound foundation, these studies often do not account for the role that the vadose zone has in delaying the arrival of draining soil water before reaching the water table. This is especially the case for past applications of regional groundwater flow models in the western United States (Rossman and Zlotnik, 2013). Moreover, GR_a rates, when estimated as deep drainage (i.e., GR_p) are only accurate in time under steady-state climatic conditions, or when depth to groundwater is relatively small (less than ~5 m; Kollet and Maxwell, 2008). Otherwise, estimates of GR_p should not be regarded as GR_a. Therefore, in determining GR_a rates one must make a proper adjustment for the lag time of soil moisture traversing the vadose zone. This is in contrast to many previous studies focusing on water quality issues, and thus on solute movement in the vadose zone (e.g., McMahon et al., 2006; Schwartz, 2006; Sousa et al., 2013).

In order to determine the lag time of soil moisture (rather than solutes), some studies perform numerical simulations of vadose zone processes on regional or basin scales by solving the nonlinear 3D Richards equation and resorting to parallel supercomputing to reduce model execution times (e.g., Kollet and Maxwell, 2008; Kollet et al., 2010). Long model execution times may lead to complications during model calibration and sensitivity analysis (Brunner et al., 2012; Hill, 2006). A simplified treatment of flow dynamics in the vadose zone involves reducing the Richards equation to 1D format and neglecting soil moisture diffusivity, i.e., gravity-driven kinematic wave approach. Implementations include the MODFLOW Unsaturated-Zone Flow (UZF1) Package (Niswonger et al., 2006) and an option in MikeShe (Graham and Butts, 2005).

Recent multi-model assessments of climate change impacts call for increased accuracy of water resource predictions through improved hydrological model development (e.g., Allen et al., 2010; Schewe et al., 2013). However, complexity of the unsaturated flow models must be consistent with the ability to measure or estimate *GR* rates and vadose zone hydraulic parameters. The saturated hydraulic conductivity, the most important of the various hydraulic parameters (Stephens, 1995), can vary by orders of magnitude depending on geologic heterogeneity. Grismer (2013) states, "determination of *GR* rates and lag times to groundwater supplies at depth remains an iterative process that includes model and estimate refinement as additional information is developed." In fact, a very small number of regional-scale hydrological modeling studies that include the vadose zone have attempted to match soil pressure heads or water contents during calibration, and constraints from these measurements do not result in uniqueness of parameter values (Brunner et al., 2012). Additionally, in an evaluation of the source of uncertainties in future *GR* estimates in Australia, Crosbie et al. (2011) found that the choice of hydrological model is the source of the least uncertainty when compared against uncertainties due to choice of Global Climate Model (GCM) and downscaling method.

The simplified approach to modeling the vertical movement of moisture through the vadose zone has been investigated by Philip (1957), Warrick et al. (1971), Wilson (1974), Sisson et al. (1980), Wilson and Gelhar (1981), Smith (1983), Rasmussen (2001), and Cook et al. (2003), among others. In contrast to tracer-based advective velocity, these studies calculate lag times using the velocity of the capillary pressure wave response due to a small perturbation of hydrologic conditions in a uniformly wetted soil profile. Following this type of approach, we investigate the hydrological effects of changing 21st century climate (as the difference between *P* and *ET*) and vadose zone thickness on vadose zone velocity and lag time and the associated timing of changes to GR_a at the water table. In this way, we address the desired high resolution, large scale (>10^5 km^2) simulation of soil moisture movement without resorting to parallel supercomputing, commonly involved in variably-saturated 3D numerical modeling of basin hydrology. We utilize published, spatially distributed, high accuracy and high resolution (1.1-km) estimates of *GR* rates based on long-term (10 yr) MODerate resolution Imaging Spectroradiometer (MODIS) satellite measurements, rather than upscaling results of point-scale vadose zone modeling as done in previous studies (e.g., Allen et al., 2010; Crosbie et al., 2010, 2013).

In this article, we propose a simple approach for estimating spatially distributed vadose zone lag times associated with long-term averaged (decadal) climate conditions over large areas. We demonstrate an application of the approach where the aim is to answer the following four related research questions about vadose zone hydrology with regard to the Nebraska Sand Hills: (1) What is the effect of a heterogeneous vadose zone thickness on the spatial distribution of vadose zone lag times? (2) How does soil hydraulic parameter uncertainty affect vertical velocity and vadose zone lag time estimates? (3) How are 21st century climate change projections expected to impact GR_p rates and vadose zone lag times? and (4) What is the percentage of surface area expected to experience changes in GR_a rates over time scales of 10, 50 and 100 years, typical of water planning and future climate modeling time scales?

2. Study area

The Nebraska Sand Hills (NSH; Fig. 1) is the largest dune region in the Western Hemisphere, with an area of ~50,000 km^2 (Loope and Swinehart, 2000). The region is characterized by a repeating pattern of native grass-stabilized sand dunes adjacent to lakes and wetlands in interdunal valleys, with a highly variable surface topography and vadose zone thickness (Bleed and Flowerday, 1998), causing lag effects to be extremely important in considerations of the spatio-temporal analysis of GR_a (Fig. 2). Diffuse *GR* within dunes supplies the groundwater system with water that eventually discharges to rivers and more than 1500 perennial lakes (Rundquist, 1983) in hydraulic connection with the unconfined aquifer system (Chen et al., 2003). Most of the lakes are considered to be groundwater sinks because *ET* exceeds *P* and a net groundwater influx makes up for the difference (Chen and Chen, 2004; Zlotnik et al., 2010). Lake and wetland areal density is the highest in the western part of the NSH where significant natural drainage features or river valleys are absent (Figs. 1 and 3). This was caused by the mobilization of sand dunes causing paleovalleys to dam during several prolonged drought periods in the Holocene (Loope et al., 1995).

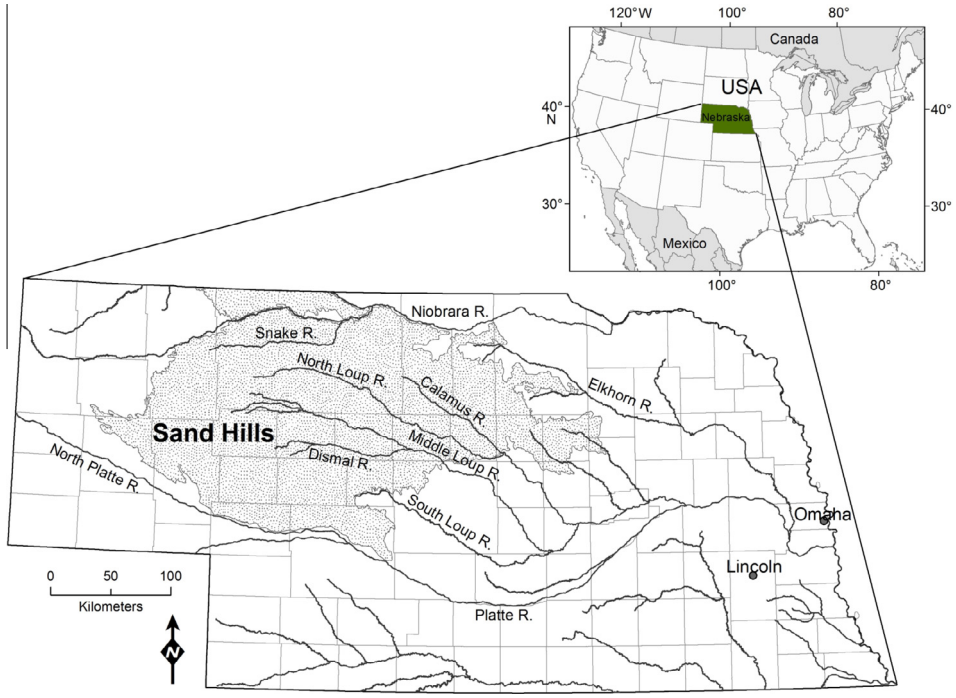

Fig. 1. The Nebraska Sand Hills, including major rivers. Thin lines are county boundaries. Rivers digital data after USGS (2010).

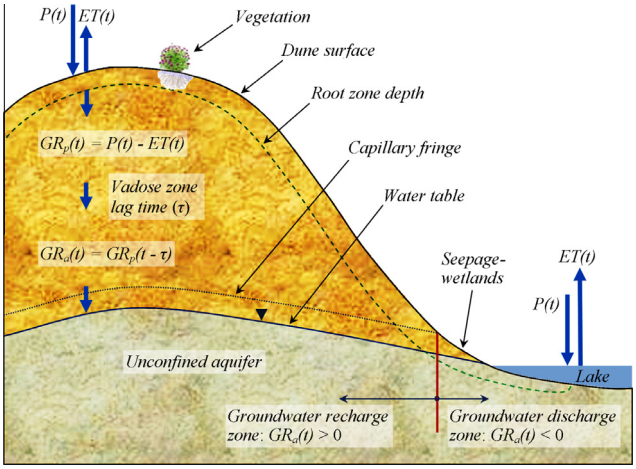

Fig. 2. Conceptual diagram illustrating the hydrology of dune areas (groundwater recharge zones) and interdunal valleys (groundwater discharge zones) in the NSH, including GR_p (deep drainage beneath the root zone), and GR_a (flux across the water table), after some vadose zone lag time (τ), where t is time.

Dunes in the NSH are composed of eolian sand that is well-sorted, and fine-to-medium grained (Sweeney and Loope, 2001). Thus, soils in the region have sand content close to 100% in some locations (NRCS, 2006; Strassberg et al., 2009). Due to the high hydraulic conductivity of the sandy soils and limited precipitation in the semi-arid environment (450 mm/yr in the western-most part to 650 mm/yr in the eastern-most part), infiltration rates are high and overland flow is minimal (Bleed and Flowerday, 1998; Szilagyi et al., 2003). In the NSH, Holocene sand deposits overlie up to 300 m of Quaternary and/or Pliocene alluvial sand and silt (Wang et al., 2009) and coarse clastic sediments of the Miocene Ogallala Group, that all-together make up the thickest part of the High Plains aquifer (Loope et al., 1995). The High Plains aquifer is considered a vital source of water for irrigated agriculture in the central United States, leading the NSH to be regarded as one of its most important *GR* areas (Szilagyi et al., 2011b).

Groundwater recharge rates in the NSH can be large and have been estimated to be greater than 200 mm/yr in some locations (Szilagyi et al., 2011b). These high rates of *GR*, along with a large groundwater reservoir (High Plains aquifer), make the region economically as well as ecologically valuable, supplying water to major rivers, thousands of groundwater fed lakes and wetlands, and sub-irrigating meadows—responsible for a third of Nebraska's beef cattle industry (Gosselin et al., 2000). The region is unique ecologically for its relatively natural state and biodiversity (Harvey et al., 2007), as most of the region is either undeveloped or used only for grazing livestock (Peterson et al., 2008). If *GR* were to be reduced because of extended and/or severe drought, as has happened in the geologic past (Loope et al., 1995; Mason et al., 2004; Schmieder et al., 2011), the water table would be lowered and discharge to lakes and rivers would be significantly decreased (Chen and Chen, 2004), threatening the existence of the region's unique and valuable ecosystems and much of its economic value.

3. Methods

3.1. Vadose zone thickness

Calculating vadose zone lag time requires estimates of the thickness of the vadose zone, or depth to the water table (D_{wt}). The vadose zone thickness was estimated as a difference between land surface and water table elevations with consideration of surface water bodies.

A map of D_{wt} was created using ArcGIS™ as the difference in elevations from a 30-m digital elevation model (DEM) of land surface topography (USGS, 1999) and a regional water table map generated in this study. The water table map was converted into a continuous field using a spline interpolation of vertices from 1995 digital water table contours (Summerside et al., 2001) and an appended point layer of lakes and rivers (USGS, 2010) with elevations extracted from the DEM of land surface topography.

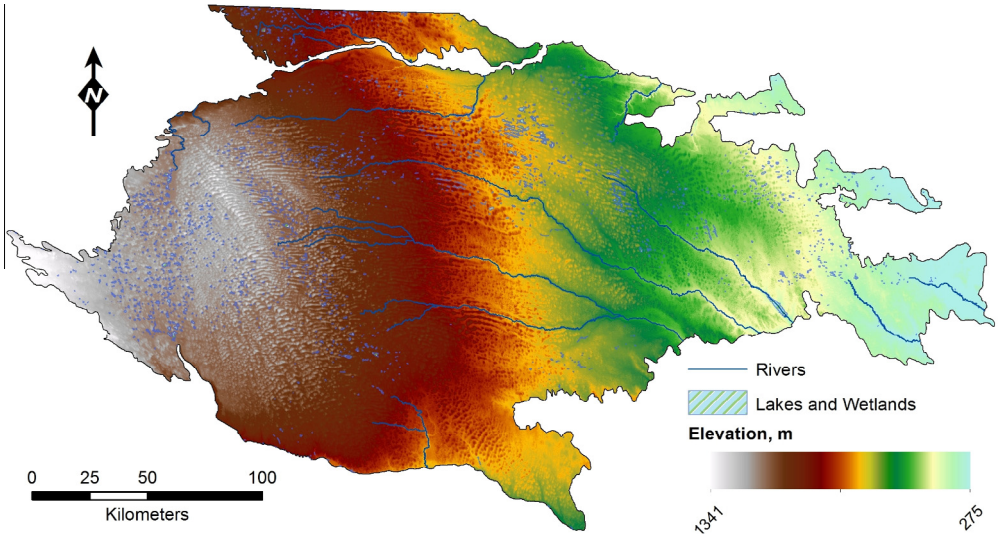

Fig. 3. Land surface topography of the NSH, including major rivers, lakes and wetlands. 30-m digital elevation model data after USGS (1999). Rivers, lakes and wetlands digital data after USGS (2010).

A conditional statement was used to make all negative values in the resulting dataset equal to zero (since negative vadose zone thickness cannot physically exist). Then the 30-m resolution dataset of D_{wt} was aggregated to 120-m (using the ArcGIS™ spatial join by location tool with mean values) in order to reduce the total number of data points, making calculations possible during the next step in the analysis in which vadose zone thickness within each 1.1-km pixel of MODIS-derived (2000–2009) potential *GR* rates ($GR_{p,\mathrm{MODIS}}$) is required, allowing for the estimation of spatially distributed vadose zone lag times (described in Sections 3.2 and 3.3). Mean D_{wt} (120-m aggregated) within each $GR_{p,\mathrm{MODIS}}$ pixel was utilized in calculations of vadose zone lag times. Descriptive statistics (mean, min., max., count (N), standard deviation (σ)) of the D_{wt} variable within each $GR_{p,\mathrm{MODIS}}$ pixel (81–100 D_{wt} values each) were also calculated to quantify the variability of D_{wt} estimates.

Depth to the water table within each 1.1-km pixel differs from the mean value due to the variability of the terrain and water table. In general, spatial variability of the water table is smaller than for the land surface elevations, and it is assessed on the order ±1 m since it was created using accurate land-based surveys and data interpolated and published by Summerside et al. (2001). However, the water table variability within a 1.1-km pixel may reach values similar to the variations in the land surface elevations near lakes in the western Sand Hills (Ong, 2010). We assessed the variability of D_{wt} within $GR_{p,\mathrm{MODIS}}$ pixels by calculating the spatial average standard deviation of D_{wt}; across the entire NSH (40,291 pixels), it is ±8 m. One should note that the measurement error (vertical error) for land surface topography for each 30-m DEM pixel can reach ±5 m Holmes et al. (2000). Considering the large height of dunes in the NSH (up to 152 m), the range of variability associated with averaged D_{wt} over 1.1-km pixels for representation of the vadose zone thickness in this area is reasonable and of adequate accuracy for this study.

Values of D_{wt} were assumed to remain the same over the entire period of study (2000–2099). This assumption has the potential to add relatively small errors to estimates of vadose zone lag time since a changing climate will likely lead to changes in the configuration and elevation of the water table. However, regional water table elevations have not changed significantly in the NSH for at least the past 60 years (the entire historic observational record), from 1950 to 2009 (McGuire, 2011), and any future changes are likely to compare in magnitude with the uncertainties in the datasets used to derive D_{wt} and are likely to be much smaller than the average thickness of the vadose zone.

3.2. Estimating potential groundwater recharge rates

3.2.1. Modern period

Here we use previously published (Szilagyi and Jozsa, 2013) remote sensing-based, spatially distributed and high resolution (1.1-km) estimates of GR_p rates for the modern period (2000–2009). These potential *GR* rates ($GR_{p,\mathrm{MODIS}}$) are estimated as the difference between mean *P* (PRISM Climate Group, 2012) and MODIS-based *ET* (Fig. 4), by taking advantage of the fact that overland flow is minimal in the NSH. A water balance approach is used, which states *P*–*ET* is equal to the change in water storage at the zero-flux plane (Healy, 2010), consistent with the approach applied by Munch et al. (2013). In this approach, monthly $GR_{p,\mathrm{MODIS}}$ fluxes are averaged over a suitably long 10-yr period, making total subsurface storage changes negligible (i.e., steady-state). The technique uses basic climate data, including *P*, air temperature, humidity, global radiation, and MODIS-based monthly aggregated 8-day average daytime surface temperature values. The temperature values are subjected to a linear transformation into *ET* values based on the application of the Priestley and Taylor (1972) equation in combination with the complementary relationship (Bouchet, 1963) of evaporation, as formulated by the Morton et al. (1985) WREVAP program. This is one of the most widely tested areal *ET* estimation tools available (see Szilagyi and Jozsa, 2013; Szilagyi et al., 2003 and references therein, Szilagyi et al., 2011a, 2011b). The $GR_{p,\mathrm{MODIS}}$ rates derived from this technique are considered as net *GR* estimates, and it is possible to obtain negative values where *ET* is consistently larger than *P*. When averaged over 10 years, these areas are generally considered to be groundwater discharge zones (see Figs. 2 and 4). Since groundwater discharge zones correspond to areas with a shallow water table of less than ~5 m, known as the critical depth or extinction depth (see Chen and Chen, 2004; Kollet and Maxwell, 2008; Szilagyi et al., 2013), and relatively short vadose zone lag times, the lag times presented in this study are only for positive net *GR* zones (i.e., dune areas with $GR_{p,\mathrm{MODIS}} > 0$).

The MODIS-based technique provides $GR_{p,\mathrm{MODIS}}$ estimates with an expected error range of 15% (based on 5% error in *P*, and 10% error in *ET* rates), not unusual for field-based *GR* estimates, and is considered to be acceptable for many applications including regional groundwater modeling (Szilagyi et al., 2011b). However, mean decadal *ET* values from Szilagyi and Jozsa (2013) have been slightly corrected to account for about 8% overestimation based on a multi-year/multi-site energy balance Bowen ratio. While the use of the

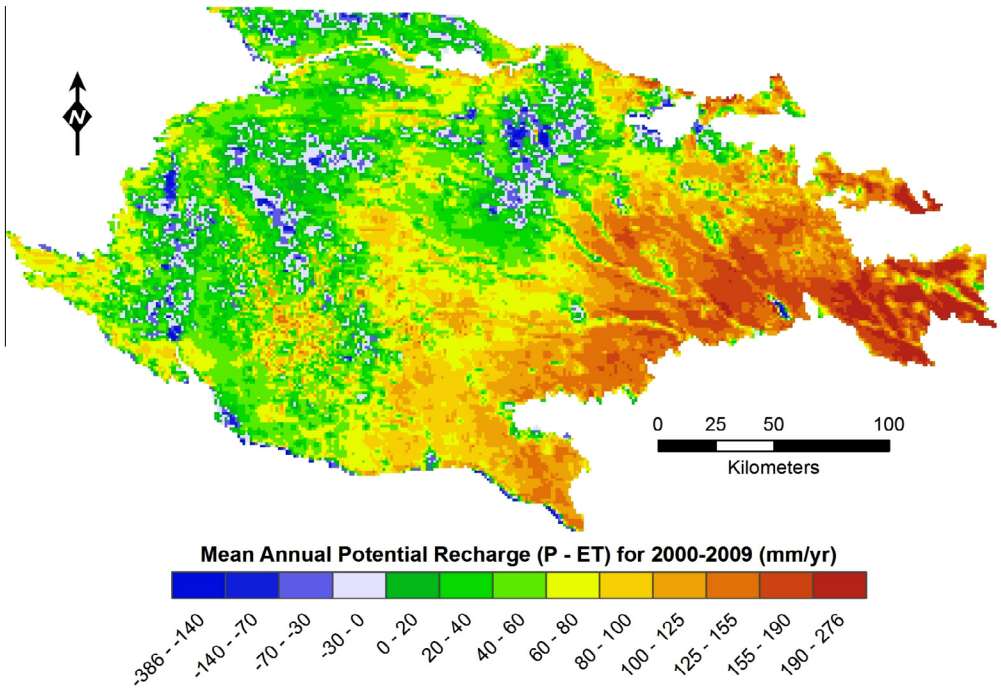

Fig. 4. Mean GR_p (mm/yr) to (and discharge from) the groundwater system in the NSH, estimated as the difference in modern period (2000–2009) mean *P* and *ET* rates. Digital data after Szilagyi and Jozsa (2013).

P–ET approach assumes any changes in soil moisture are negligible, it is very accurate with regard to the water balance partly because it captures the effects of the plant root zone with a monthly temporal resolution. Thus, the long-term estimates of deep drainage ($GR_{p,MODIS}$) are influenced by the effects of root zone soil moisture changes during wet and dry parts of the year. The resulting $GR_{p,MODIS}$ rates for the NSH have been verified by comparison with *GR* estimates using groundwater chloride mass balance and basin runoff analyses, and they have an unprecedented spatial resolution for distributed *GR* estimates in the region (Szilagyi et al., 2011b). All *P – ET* estimates are within 36 mm/yr (7% of mean *P*) for basin runoff analyses in three NSH watersheds, and within 1 mm/yr for the chloride mass balance estimates (Szilagyi et al., 2011b).

3.2.2. Future period

Changes in future period (2010–2099) GR_p rates were developed from two sets of bias-corrected spatially downscaled hydroclimate projections from the World Climate Research Programme (WCRP) Coupled Model Intercomparison Project Phase 3 (CMIP3). Data are from the U.S. Bureau of Reclamation (USBR, 2011) with hydrology variables produced using the Variable Infiltration Capacity (VIC) macroscale hydrology model (Liang et al., 1994). These hydroclimate scenarios are referred to herein as CMIP3/VIC scenarios. These data were downloaded from the U.S. Bureau of Reclamation website (http://gdo-dcp.ucllnl.org/downscaled_cmip_projections), containing monthly archives of both climate and hydrology variables from a large number of GCM results. CMIP3, rather than CMIP5, model data were used to enable comparisons to previous work and because hydrology projections were not yet available for CMIP5 at the time of writing of this article. In fact, CMIP5 climate projections change little from CMIP3 projections for the central Great Plains region of the U.S., and thus for the NSH (Brekke et al., 2013).

From the U.S. Bureau of Reclamation archive, we used the GCM produced climate variable *P* and the VIC produced hydrology variable *ET* in order to calculate (as an intermediate step) mean GR_p rates for each decade in the future period (2010–2019, 2020–2029, …, 2090–2099). Specifically, we used two GCM scenarios, including SRES-B1-NCAR-CCSM-3-0.4 (from the National Center for Atmospheric Research), and SRES-A1B-GFDL-CM2.1 (from the U.S. Department of Commerce/NOAA/Geophysical Fluid Dynamics Laboratory). These two GCMs perform relatively well in terms of their skill in reproducing observations of temperature and *P* (Knutti et al., 2013). However, visual inspection of plotted mean decadal CMIP3/VIC scenario GR_p rates in the NSH for the modern period (2000–2009) from all 36 available GCMs forced by the SRES A2 greenhouse gas emissions path (the highest global warming scenario; see IPCC, 2000), revealed a weak overall correlation with and spatial bias as compared against the $GR_{p,MODIS}$ dataset. Especially concerning is the fact that none of the CMIP3/VIC scenarios show negative GR_p rates within the NSH, even though they occur in 8.5% of pixels from Szilagyi and Jozsa's (2013) MODIS-based product, and the magnitude of the negative $GR_{p,MODIS}$ rates exceeds 300 mm/yr in some of the pixels (see Fig. 4). The poor relationship between GR_p rates from these different products ($GR_{p,CMIP3/VIC}$ vs. $GR_{p,MODIS}$) is due primarily to two reasons, including limited observational data in the NSH in which the statistical downscaling of the GCM results is based upon, affecting the accuracy of the climate model variable *P*, and the use of the VIC macroscale hydrology model to simulate *ET*. The VIC model does not adequately treat groundwater interactions with surface water because of its model structure and relatively large cell size (~12-km), leading to a very poor calibration to streamflows in and surrounding the NSH (USBR, 2011).

Because of the large discrepancy between these two GR_p datasets, we opted to use a modified "*Delta*" method implemented by the U.S. Bureau of Reclamation (USBR, 2010), and follow the approach similar to Crosbie et al. (2013) in presenting future climate change results as changes in GR_p. With this method, adjustments are made to the modern period (2000–2009) $GR_{p,MODIS}$ rates based on relative changes projected by the CMIP3/VIC scenarios as recharge scaling factors (*RSF*s). The assumption is that by calculating climate change signals from the CMIP3/VIC model simulations and applying these changes to the observed climate,

the effect of bias in the future projections is minimized. In this way, the method preserves nearly the same spatial pattern and the exact same resolution of $GR_{p,MODIS}$ estimates. To do this, we utilized the ratio of future period (2010–2099) to modern period (2000–2009) GR_p from the CMIP3/VIC scenarios. Thus, for the future decades (t), *RSF*s were calculated as $RSF(t) = GR_p(t)/GR_p(2000–2009)$. Then, the dataset of $GR_{p,MODIS}$ values were multiplied by $RSF(t)$ to obtain future annual potential *GR* averaged over time t ($GR_p(t)$). This was done for each $GR_{p,MODIS}$ pixel and each future decade (from 2010 to 2099) for both a wet and dry future GCM scenario.

While only two CMIP3/VIC scenarios are utilized in this study (wet and dry), their method of selection allows for the representation of the uncertainty range in projections of changes in GR_p rates for a 2090–2099 climate relative to a 2000–2009 climate, due to different magnitudes of global warming by the end of the 21st century and differences among GCMs and greenhouse gas emission paths. This was accomplished by first calculating the sample standard deviations of the spatially averaged *RSF*s (mean for 2090–2099) from all 112 available CMIP3/VIC hydroclimate model runs (including 16 GCMs and 3 emission paths) in the NSH. Then, the two hydroclimate scenarios with *RSF*s nearest to $\pm1\sigma$ from the mean were selected. We found the scenario nearest to $+1\sigma$ (SRES-B1-NCAR-CCSM-3-0.4) and the scenario nearest to -1σ (SRES-A1B-GFDL-CM2.1) from the mean of the 112 spatially averaged *RSF*s. These were defined as wet and dry scenarios, respectively.

A more rigorous evaluation quantifying uncertainty due to these scenarios would explicitly include all 112 available hydroclimate projections in the calculation of vadose zone lag times, and would examine other sources of uncertainty, such as caused by statistical downscaling and the use of the VIC hydrology model. This would require an unnecessarily long amount of time, and the resulting *RSF*s obtained from this approach are similar in magnitude to those presented by Crosbie et al. (2013) for the Northern High Plains (which encompasses the NSH region).

3.3. Vertical velocity and lag time of soil moisture

There are three major velocity characteristics of soil moisture in the vadose zone with a unit hydraulic gradient initial profile; one is Darcy's velocity. If we assume that the movement of moisture through the vadose zone is vertical (where the vertical coordinate z increases downward), gravity-driven, and steady, such that a unit hydraulic gradient exists ($\partial H/\partial z = -1$), as is conventionally specified (e.g., Rasmussen, 2001; Sisson et al., 1980; Warrick et al., 1971), we obtain the following expression:

$$q = GR_p = K(\theta) \tag{1}$$

which states that Darcy's velocity (q) equals the potential *GR* rate (GR_p) and the water-dependent hydraulic conductivity [$K(\theta)$], where θ is the volumetric soil water content, and H is the total hydraulic head.

Small perturbations of hydrologic conditions at the land surface result in similarly small changes of soil moisture contents and pressure (or pressure gradients) traveling downward with the vertical velocity (c) as follows:

$$q = \frac{dq}{d\theta} = \frac{dK(\theta)}{d\theta} \tag{2}$$

This velocity is used if one is interested in the timing of arrival of capillary pressure changes at the water table resulting from the changes in pressure and pressure gradients at the land surface (Philip, 1957; Warrick et al., 1971; Wilson, 1974), referred to as the kinematic wave approximation (Sisson et al., 1980) or kinematic velocity (Rasmussen, 2001). The pressure-based velocity is the most relevant when calculating lag times associated with *GR*. The relationship $K(\theta) = GR_p$ from Eq. (1) can also be used to infer spatially distributed, but vertically averaged θ values in pixels where GR_p and soil hydraulic parameters are specified.

Finally, a conservative tracer-based velocity (v) in the vadose zone is calculated as the advective tracer velocity using:

$$v = \frac{q}{\theta} = \frac{K(\theta)}{\theta} \tag{3}$$

which is the equation of interest for aquifer vulnerability studies (e.g., Healy, 2010).

Studies of Warrick et al. (1971), Wilson (1974), Wilson and Gelhar (1981), and Rasmussen (2001) showed that the pressure-based (kinematic) velocity exceeds the tracer-based (advective) velocity by a factor in excess of two to four, depending on moisture content, choice of conductivity–water content relation and solute transport parameters. The tracer-based velocity is greater than Darcy's velocity as follows from Eq. (3).

Considering the relative homogeneity of soil texture within sand dunes, and a previous study of numerous High Plains sites with thick vadose zones (15–50 m), in which McMahon et al. (2006) found that hydraulic gradients are near unity, ranging from 0.83 to 0.97, the assumptions used in obtaining Eq. (2) are thought to be valid for application in the NSH. The unit hydraulic gradient assumption is also valid when considering the relatively small changes in GR_p associated with the decadal time step used. However, selection of this large time step does have the potential to inflate estimates of the lag times of the draining water's center of mass, since wet periods (with duration of days to weeks) could significantly increase GR_p rates and vertical velocities (see Grismer, 2013). Thus, we consider the lag time estimates achieved with this approach as conservative (large), and recommend that it be used as a first-order approximation with a decadal (or longer) time step. The van Genuchten–Mualem equation (Mualem, 1976; van Genuchten, 1980) is used to calculate $K(\theta)$ and c, with baseline soil hydraulic parameters taken for sand from Carsel and Parrish (1988) and NRCS (2006). This equation for hydraulic conductivity is expressed as

$$K(S_e) = K_s S_e^{1/2}\left[1 - \left(1 - S_e^{1/m}\right)^m\right]^2 \tag{4}$$

and the relative saturation (S_e) as

$$S_e = (\theta - \theta_r)/(\theta_s - \theta_r) \tag{5}$$

where K_s is the saturated hydraulic conductivity; θ_r is the residual soil water content; θ_s is the saturated soil water content; and m is a pore size distribution coefficient. The equation for soil moisture vertical velocity (c) is obtained by differentiating Eq. (4) with respect to θ, expressed as

$$c = \frac{dK(\theta)}{d\theta} = \frac{K_s(1 - S_f^m)^2}{2(\theta_s - \theta_r)S_e^{1/2}}\left[1 + \frac{4S_e^{1/m}S_f^{m-1}}{(1 - S_f^m)}\right] \tag{6}$$

where

$$S_f = 1 - S_e^{1/m} \tag{7}$$

The reference to "baseline" soil hydraulic parameters is used here as they are estimates, which are known to vary at least somewhat across the NSH. Nevertheless, they are considered as current best estimates, given that field studies of soil hydraulic parameters are limited in the NSH (especially for depths below the root zone). Sensitivity analyses of the effects of soil hydraulic parameter uncertainty on the spatial mean and range of vertical velocity and lag time estimates were also conducted by systematically varying the two most sensitive and uncertain parameters, K_s and θ_r.

Once vertical velocity (c) had been determined using Eqs. (6) and (7), vadose zone lag time (τ) was computed using the following expression:

$$\tau = D_{wt}/c \quad (8)$$

where D_{wt} is the mean depth to the water table (or vadose zone thickness) described in Section 3.1. The spatial pattern of τ was mapped in ArcGIS™ by appending values of it to a point shapefile of $GR_{p,\mathrm{MODIS}}$ values, and then converting them into a raster dataset aligning with $GR_{p,\mathrm{MODIS}}$ pixels. Values of c and τ were calculated only for positive $GR_{p,\mathrm{MODIS}}$ pixels (36,663 pixels, ~44,600 km^2), representative of upland net GR zones (see Fig. 2), because lag times should be small and can be neglected for zones with net groundwater discharge ($GR_{p,\mathrm{MODIS}} < 0$).

The methods used here to estimate D_{wt} may lead to an overestimation of lag times because the effects of capillary rise near the water table and thickness of the root zone are not taken into account (i.e., D_{wt} is considered to be the difference between the land surface and the water table elevations). However, in general, these factors will likely lead to only small errors in lag time estimates, and potential errors arising from these factors would be largest where the water table is relatively shallow and smallest where the water table is relatively deep.

4. Results and discussion

4.1. Vadose zone thickness in the NSH

The tremendous spatial variability of topography in the NSH (Fig. 3) causes considerable changes in vadose zone thickness (D_{wt}) on local and regional scales (Fig. 5), affecting the interaction between the climate and the aquifer through ET and GR. Fig. 5 illustrates the extreme variation of D_{wt} in the NSH, which ranges from 0 to 152 m, with a mean of 21.9 m (σ = 15.6 m). Approximately 80.3% of the region (~39,000 km^2) has D_{wt} that is greater than the approximate extinction depth of 4 m (Chen and Chen, 2004; Szilagyi et al., 2013), where groundwater ET is no longer influenced by vegetation (Soylu et al., 2010). Additionally, a substantial portion of the region (35.7%, ~17,500 km^2) has $D_{wt} > 25$ m. These areas generally occur in the central and western parts of the NSH, with exceptionally large D_{wt} where there are large sand dunes, and in some areas surrounding highly incised river valleys, including two large areas near the headwaters of the Dismal and Middle Loup Rivers in the central part of the NSH (Fig. 1, and warm colors in Fig. 5). The extensive occurrence of a thick vadose zone indicates the importance of lag times for future water resources planning and climate change studies (e.g., at 10, 50 and 100 yr time scales). The spatial distribution and overall magnitude of vadose zone thickness presented here is consistent with that found within a large portion of the central NSH (~10,000 km^2) by Chen and Chen (2004), who used similar regional datasets of the land surface and water table topography.

4.2. Vadose zone lag times with modern period potential groundwater recharge

Estimates of vadose zone lag times using Eq. (8) were made for 36,663 independent $GR_{p,\mathrm{MODIS}}$ pixels in the NSH (~44,600 km^2). The large $GR_{p,\mathrm{MODIS}}$ rates (Fig. 4), with a mean of 78 mm/yr for positive $GR_{p,\mathrm{MODIS}}$ areas, along with the highly permeable sand deposits that characterize the NSH's geology, promote relatively quick drainage of vadose zone water. However, extreme variations exist in the spatial distribution of lag time estimates (Fig. 6). Comparison of Figs. 4–6 allows examination of the effect of a heterogeneous vadose zone thickness on the spatial distribution of vadose zone lag times (as influenced by modern period GR conditions). The longest vadose zone lag time estimates in the NSH (warm colors in Fig. 6) occur in areas with a deep water table (warm colors in Fig. 5) and low GR rates (cool colors in Fig. 4), and *vice versa* for the shortest lag times. Many pixels with relatively long lag time estimates in the north-central and western parts of the NSH (sand dune areas) are found directly adjacent to those with minimal lag times (areas with lakes and wetlands; see Fig. 3). Also, other areas with a thick vadose zone (besides dunes; described in Section 4.1) have relatively long (greater than the mean) lag time estimates, whereas vast areas in eastern parts of the NSH have relatively short lag time estimates due to a shallow water table and large GR_p rates.

Estimated vadose zone lag times with average modern period $GR_{p,\mathrm{MODIS}}$ rates range from 0 to 359 yrs, with a spatial mean of 5.28 yrs (assuming baseline soil hydraulic parameters; see Table 1). These lag time estimates are consistent with the range of tracer-based lag times reported by McMahon et al. (2006) of about 50–375 yrs for irrigated sites in the High Plains (with 15–50 m thick vadose zones) when one considers the relationship between pressure-based and tracer-based velocities, since solutes move by a factor of roughly two to four times slower than pressure changes in the vadose zone (Rasmussen, 2001; Wilson, 1974). Vertical velocities estimated here (mean of 5.68 m/yr, ranging from 0.24 to 14.9 m/yr), assuming baseline soil hydraulic parameters, are also consistent with those reported by McMahon et al. (2003) of at least 2–3 m/yr for an irrigated site in the Central High Plains composed of sandy and loamy soils (with an estimated deep drainage rate of 53–54 mm/yr). Furthermore, Istanbulluoglu et al. (2012) applied a linear reservoir model fitted to the North Loup watershed's (see Fig. 1) empirically determined runoff response to climate, and found a basin drainage time scale of 9.5 years, effectively representing the combined lag effects of both the vadose zone and High Plains aquifer. Their single estimate of lag time is several years longer than the mean found here for the NSH, as expected, since lag times associated with the aquifer are excluded here. Thus, our relatively simple technique yields estimates that are consistent with those from previous field and more detailed modeling studies.

4.3. Sensitivity of vertical velocity and lag time estimates to soil hydraulic parameter uncertainty

Here we focus on the sensitivity of the two most important and uncertain hydraulic parameters, saturated hydraulic conductivity (K_s) and residual soil moisture content (θ_r). The highest $GR_{p,\mathrm{MODIS}}$ rate for any pixel in the NSH is 276 mm/yr, constraining the inferred depth-averaged soil moisture content within any given $GR_{p,\mathrm{MODIS}}$ pixel to be no greater than 0.151 m^3/m^3 (based on assumptions in using Eq. (1)). Thus, the influence of varying θ_r is expected to be much larger than for θ_s (assumed to be 0.43 m^3/m^3; see Table 1). Parameter m in the van Genuchten–Mualem equation is unlikely to vary much for eolian sand, and its sensitivity with regard to changes in vertical velocity and lag time are also assumed to be small relative to those caused by variations in K_s and θ_r.

Baseline and adjusted soil hydraulic parameters used in the sensitivity analyses and their impact on the spatial mean and range of the vertical velocity (c) and vadose zone lag time (τ) estimates within the NSH (assuming mean decadal $GR_{p,\mathrm{MODIS}}$ rates) are presented in Table 1. Runs 2–5 test changes in adjustments to K_s (varied between 0.316 and 10.54 m/d), and runs 6–9 test changes in adjustments to θ_r (varied between 0.0135 and 0.0900). Baseline parameters are taken for sand from Carsel and Parrish (1988), and NRCS (2006) for K_s, in the absence of detailed field characterization of deep soils/vadose zone geology in the NSH. The range in adjusted K_s values investigated here is representative of the expected range of variation based on field work in the western part

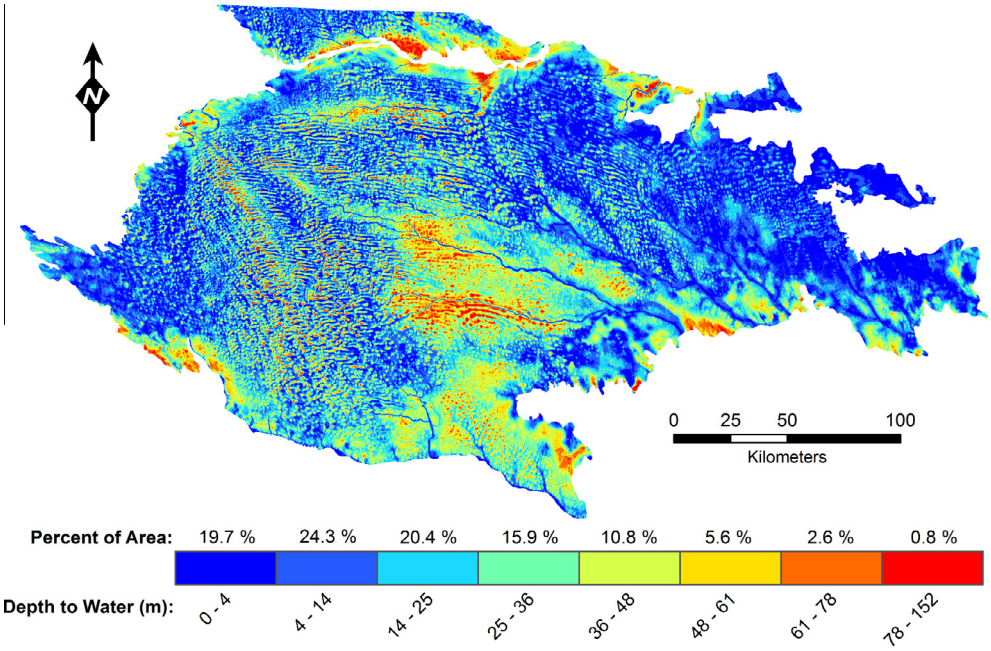

Fig. 5. Thickness of the vadose zone (m) in the Sand Hills within eight color-coded classes, estimated as the difference in 30-m digital elevation model data after USGS (1999) and spring 1995 water table digital data after Summerside et al. (2001). (For interpretation of the references to color in this figure legend, the reader is referred to the web version of this article).

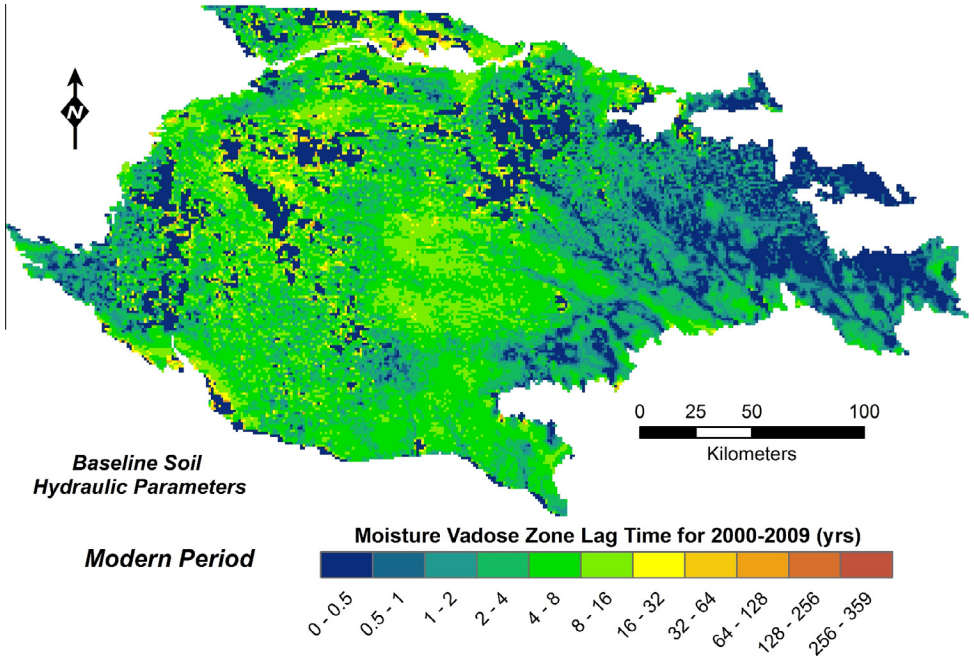

Fig. 6. Vadose zone lag time (yrs) of soil moisture in the NSH with baseline soil hydraulic parameters, estimated using vadose zone thickness and modern period averaged (2000–2009) mean $GR_{p,MODIS}$ rates. Note the logarithmic scaling of color-coded classes. (For interpretation of the references to color in this figure legend, the reader is referred to the web version of this article).

of the NSH presented by Zlotnik et al. (2007), who used direct push methods to obtain K_s measurements from three depths (exceeding several meters) at 11 sites. The range in adjusted θ_r values represents variations for sand consistent with those presented by Carsel and Parrish (1988). Testing the influence of these expected variations allows for assessment of the level of potential error arising from the uncertainty involved in soil hydraulic parameter estimates.

The largest changes in vertical velocity and lag time estimates are due to the most sensitive and uncertain soil hydraulic parameter, K_s (Table 1). Furthermore, the longest vadose zone lag time estimate of 496 yrs (mean of 7.28 years) is associated with the smallest K_s value tested (0.316 m/d); and the shortest lag time estimates (mean of 2.85 yrs, and max. of 194 yrs) is associated with the largest K_s value tested (10.54 m/d). The effects of varying K_s and θ_r independently for all nine runs (including the baseline)

Table 1
Results of sensitivity analyses of the mean and range of vertical velocity and lag time estimates within the NSH using baseline (run 1) and adjusted soil hydraulic parameters (runs 2–9).[a]

Run	K_s (m/d)	θ_r (m^3/m^3)	c		τ	
			Mean (m/yr)	Range (m/yr)	Mean (yrs)	Range (yrs)
1	1.054	0.0450	5.68	0.24–14.9	5.28	0–359
2	0.632 (−40)	0.0450	4.96 (−13)	0.21–13.0	6.05 (+15)	0–412 (+15)
3	0.316 (−70)	0.0450	4.13 (−27)	0.17–10.9	7.28 (+38)	0–496 (+38)
4	2.108 (+100)	0.0450	6.83 (+20)	0.29–17.8	4.39 (−17)	0–298 (−17)
5	10.54 (+900)	0.0450	10.5 (+85)	0.45–27.4	2.85 (−46)	0–194 (−46)
6	1.054	0.0270 (−40)	5.43 (−4)	0.23–14.2	5.53 (+5)	0–376 (+5)
7	1.054	0.0135 (−70)	5.25 (−8)	0.22–13.7	5.71 (+8)	0–387 (+8)
8	1.054	0.0675 (+50)	6.03 (+6)	0.26–15.8	4.97 (−6)	0–339 (−6)
9	1.054	0.0900 (+100)	6.43 (+13)	0.28–16.8	4.66 (−12)	0–315 (−12)

[a] Percent relative changes from the baseline are shown in parentheses. Modern period (2000–2009) mean $GR_{p,MODIS}$ rates are used. Soil hydraulic parameters are for sand from Carsel and Parrish (1988), with K_s from NRCS (2006). θ_s (0.430 m^3/m^3) and m (0.0627) are unchanged for all runs.

are shown graphically in Fig. 7, illustrating their effect on the nonlinear relationship between vertical velocity of the pressure pulse and soil moisture content, based on the proposed 1D pressure-based approach. Fig. 7 also shows the expected range in soil moisture content in positive net *GR* zones (where $GR_{p,MODIS} > 0$), which varies from 0.030 to 0.151 m^3/m^3 (the range on the *x*-axis), and that the estimated vertical velocities do not exceed 27.4 m/yr (the max. value on the *y*-axis). Although, for individual combinations of K_s and θ_r, the predicted range in θ and c is smaller than that shown in Fig 7. While the possible range of vertical velocities is shown to vary substantially in Fig. 7, the impacts of the uncertainty due to K_s and θ_r does not lead to the same relative changes in estimated mean lag times as they do for mean vertical velocities (see Table 1). In fact, the degree of sensitivity to K_s decreases with increasing K_s values for the mean τ relative to the sensitivity of the mean c. This is caused by the mediating factor of D_{wt} used in calculating lag times, and the fact that the degree of sensitivity of vertical velocity to K_s is a function of θ, and that sensitivity decreases with decreasing θ, whereas the degree of sensitivity to θ_r does not vary with θ (Fig. 7). Although, the sensitivity of θ_r does also appear to vary in direction depending on the predicted variable (c or τ).

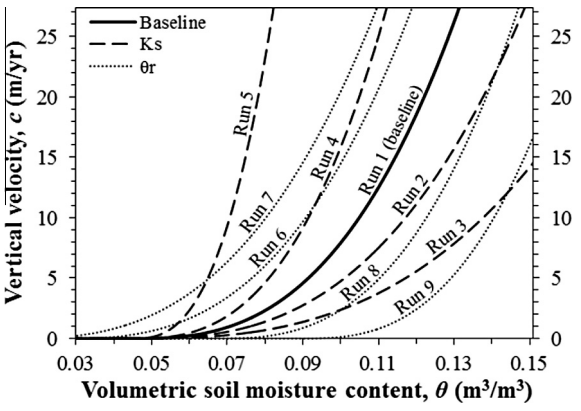

Fig. 7. Relationship between vertical velocity (m/yr) and soil moisture content (m^3/m^3) with baseline and adjusted soil hydraulic parameters presented in Table 1.

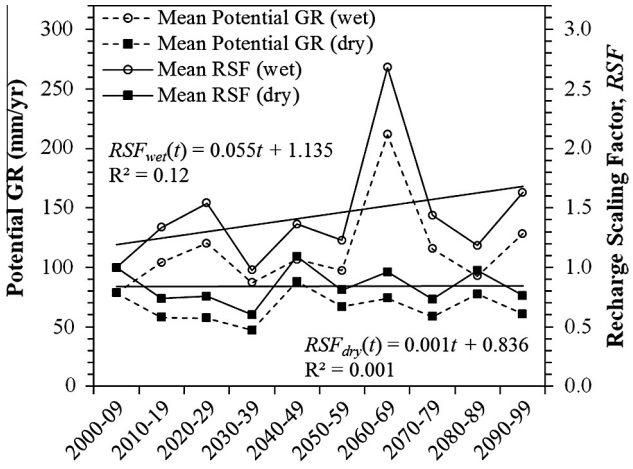

Fig. 8. Modern period (2000–2009) and projected future period (2010–2099) spatially averaged mean GR_p rates (mm/yr) and mean *RSF*s by decade for both wet and dry hydroclimate scenarios in the NSH, including linear trend lines of *RSF*s, where t is time in decades.

4.4. Vadose zone lag times with future period potential groundwater recharge

The effects of the two future climate change scenarios investigated (wet and dry CMIP3/VIC scenarios), on spatially averaged 10-yr GR_p rates in the NSH, differ by both magnitude and direction of changes relative to the modern period (Fig. 8). Also, GR_p rates in the future period (2010–2099) exhibit moderate (dry scenario) to high (wet scenario) interdecadal variations (Fig. 8). The wet hydroclimate scenario produces a spatially averaged future period (2010–2099) mean *RSF* of 1.49, which translates into a mean GR_p rate of 118 mm/yr over the NSH. By the end of the century (2090–2099), the decadal GR_p rate under a wet future climate is projected to be 128 mm/yr (*RSF* = 1.63), an increase of 50 mm/yr relative to the modern period (2000–2009). Additionally, the largest variation for a single decade in the wet scenario produces the highest projected spatially averaged GR_p rate of 212 mm/yr (*RSF* = 2.68), occurring in the decade of 2060–2069. In contrast, the dry hydroclimate scenario produces a spatially averaged future period mean *RSF* of 0.82, translating into a mean GR_p rate of 65 mm/yr. By the end of the century (2090–2099), the spatially averaged 10-yr mean GR_p under a dry future climate is projected to be 61 mm/yr (*RSF* = 0.76), a decrease of 17 mm/yr relative to the modern period. In addition, the lowest projected mean GR_p rate, occurring in the decade of 2030–2039, is 47 mm/yr (*RSF* = 0.60). Thus, there is considerable uncertainty in the magnitude and direction of projected groundwater recharge changes for the NSH, since the two future scenarios are representative of $\pm 1\sigma$ from the mean *RSF* of 1.21 (N = 112).

The NSH mean $GR_{p,MODIS}$ rate, and wet and dry scenario *RSF*s for 2090–2099 are: 78 mm/yr, 1.63, and 0.76, respectively (for pixels where $GR_{p,MODIS} > 0$). These values are comparable to those found by Crosbie et al. (2013) for the Northern High Plains region (which

encompasses the NSH), despite the differences in methodology used to estimate GR_p and future *RSF*s. They modeled a spatially averaged mean GR_p rate of 78 mm/yr for the historical period (1982–2011), and future (2050) *RSF*s of 1.32 and 0.76 with GCM climate variables used as input to the Soil-Vegetation-Atmosphere-Transfer model, WAVES, and upscaling of results with the aid of regional soil texture and vegetation datasets. The fact that the *RSF*s calculated by Crosbie et al. (2013) were for year 2050 might explain some of the difference between their wet scenario *RSF* and that found here of 0.31 (ΔRSF = 1.63–1.32), as the wet scenario analyzed in this study has a mean *RSF* of 1.30 for the 2040–2060 period. However, the 2040–2060 mean *RSF* for the dry scenario is 0.95 here, a value of 0.19 larger than that reported by Crosbie et al. (2013) for 2050. For future GR_p scenarios in the NSH, we thus conclude that interdecadal variations in *RSF*s between GCM scenarios are large, adding to some of the observed deviations in *RSF*s throughout the 21st century. This is evident because Crosbie et al. (2013) used average results of 16 GCMs, while only one GCM scenario was used here for each of the two hydroclimate scenarios. Yet, the historical mean and overall trends in future spatially averaged mean GR_p rates found here are comparable to those found by Crosbie et al. (2013). However, an important distinction is that the spatial distribution of future *RSF*s from this study are substantially different than those found by Crosbie et al. (2013). This is explained by the utilization of the "*Delta*" method here, rather than aggregated estimates of GR_p from point-scale modeling. That is why the spatial distribution of future GR_p rates found in this study still greatly reflects that from the MODIS-based estimates of Szilagyi and Jozsa (2013), which is most likely a more accurate representation of the spatial distribution of GR_p.

Figs. 9 and 10 illustrate the spatial distribution of vadose zone lag time with mean end-of-century (2090–2099) GR_p rates (wet and dry scenarios, respectively). The wet and dry future GR_p scenario spatially averaged end-of-century (2090–2099) mean (max.) vadose zone lag time estimates are 3.78 yrs (583 yrs) and 6.55 yrs (253 yrs), respectively (assuming baseline soil hydraulic parameters; see Table 1). This represents a change in the mean (max.) vadose zone lag times by −29% (−42%) and +24% (+30%) for the wet and dry scenarios, respectively. However, the large *RSF* for the wet scenario, with a spatial mean over the NSH of 1.63 (representing a 63% increase in GR_p for 2090–2099 relative to 2000–2009), does not translate into the same magnitude of changes in estimated lag times. This is partly attributed to the spatial bias in the future wet CMIP3/VIC hydroclimate scenario GR_p rates, because they systematically predict greater increases in GR_p for the northern and western parts of the NSH. These areas have low $GR_{p,MODIS}$ rates and make up a large proportion of the pixels with long lag times.

A particularly interesting finding is that the entire histogram of vadose zone lag time estimates for the 2090–2099 period is shifted relative to those with 2000–2009 $GR_{p,MODIS}$ rates (Fig. 11). The wet scenario shifts the histogram toward shorter lag times, while the dry scenario shifts the histogram toward longer lag times. Additionally, analysis of cumulative frequency curves of vadose lag time estimates within the NSH (Fig. 11) provides estimates of the percentage of NSH area expected to experience changes in GR_a rates over any time scale (equal to the vadose zone lag time of interest). With modern period mean $GR_{p,MODIS}$ rates, most of the NSH groundwater system surface area (89.9%) is expected to reflect changes in GR_a from changing climatic conditions within 10 years (by 2019), and nearly all of it within 50 years (99.6% by 2059), and 100 years (99.9% by 2099).

For comparison, with future GR_p rates (2090–2099), 99.8% (wet scenario) and 99.4% (dry scenario) of the NSH groundwater system surface area is estimated to be affected by changes in the GR_p rate within 50 years (by 2059). This translates into a change in the area affected by only ±85 km^2 (relative to 2000–2009). Compared to the large changes in the mean estimated vadose zone lag time in response to changes in GR_p rates under future hydroclimate scenarios (−29% and +24%), the expected changes at the tail end of the distribution are relatively small (notice the convergence of cumulative frequency curves for large lag times in Fig. 11).

Since only a small portion of the NSH has estimated vadose zone lag times exceeding 10 years, changes in GR_a that differ from GR_p rates, for the same decade, are not predicted to be drastic

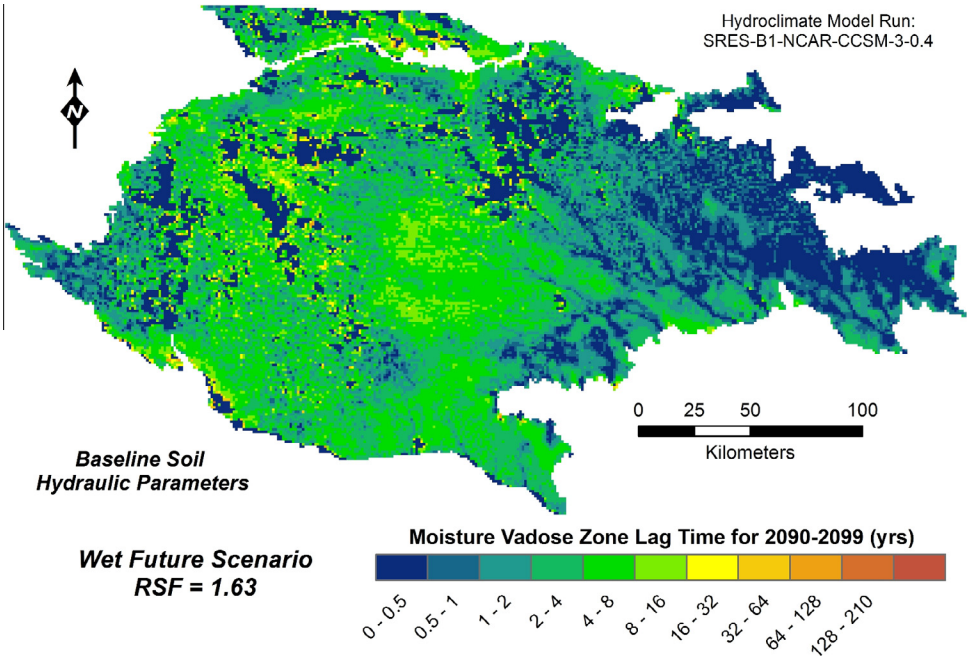

Fig. 9. Vadose zone lag time (yrs) of soil moisture in the NSH under the wet hydroclimate scenario with baseline soil hydraulic parameters, estimated using vadose zone thickness and end-of-century (2090–2099) mean GR_p rates (spatial mean *RSF* of 1.63). Note the logarithmic scaling of color-coded classes, and that the scale is the same as that of Fig. 6. (For interpretation of the references to color in this figure legend, the reader is referred to the web version of this article).

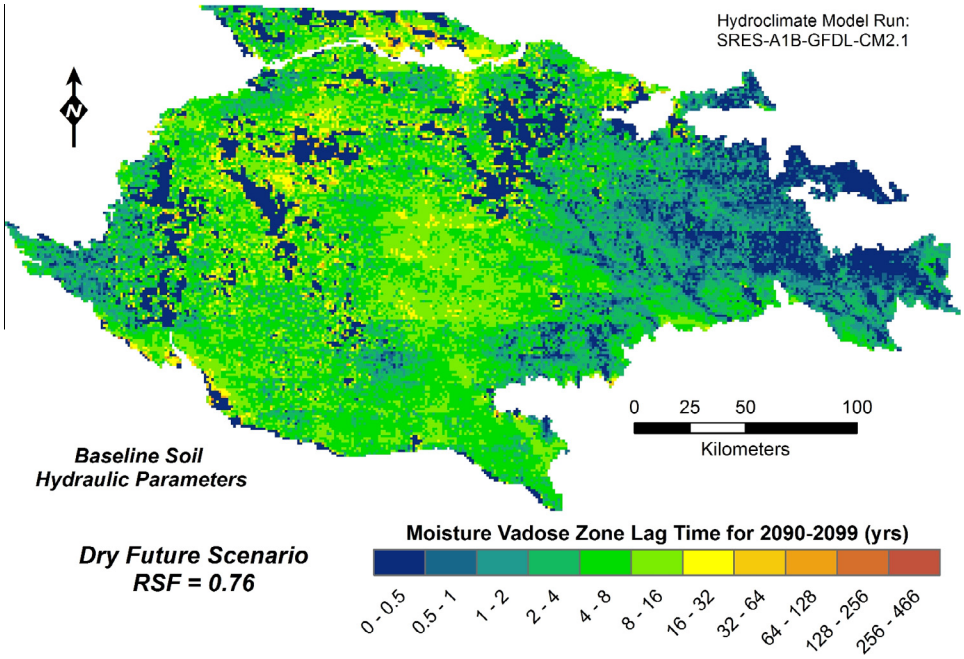

Fig. 10. Vadose zone lag time (yrs) of soil moisture in the NSH under the dry hydroclimate scenario with baseline soil hydraulic parameters, estimated using vadose zone thickness and end-of-century (2090–2099) mean GR_p rates (spatial mean *RSF* of 0.76). Note the logarithmic scaling of color-coded classes, and that the scale is the same as that of Figs. 6 and 9. (For interpretation of the references to color in this figure legend, the reader is referred to the web version of this article).

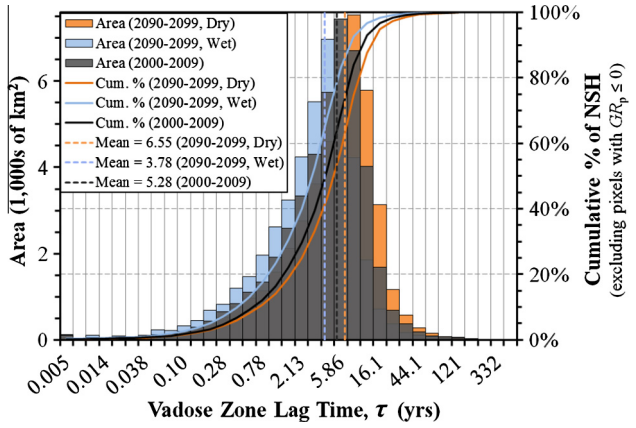

Fig. 11. Histograms and cumulative frequency curves of vadose zone lag time estimates (yrs) in the NSH for 2000–2009 using $GR_{p,MODIS}$ rates, and 2090–2099 wet and dry hydroclimate scenarios using CMIP3/VIC adjusted GR_p rates. Baseline soil hydraulic parameters are used. Dotted vertical lines are mean lag times for the modern period and both future hydroclimate scenarios.

throughout the entire 21st century. The longest estimated future mean vadose zone lag times in the NSH (assuming baseline soil hydraulic parameters) occur when the GR_p in the dry scenario drops to a low of 47.2 mm/yr in the decade of 2030–2039 (from 78 mm/yr for 2000–2009), with a corresponding mean lag time of 7.7 years. During that decade, ~75% of the NSH is expected to have lag times shorter than 10 years. Also, interdecadal variability in GR_p rates for the dry scenario future climate are considered moderate—mean annual GR_p rates range from 47.2 mm/yr to 88.0 mm/yr, while the mean for the entire future period (2010–2099) is 65.4 mm/yr (Fig. 8).

These findings provide evidence that for groundwater modeling applications in the NSH, changes in GR_p can be used as input without explicitly accounting for vadose zone lag times only if the interest lies in utilizing stress periods with a temporal resolution of approximately a decade, or longer. However, lag times will not be the same in other regions, and for many applications shorter stress periods in models will be needed. Therefore, the proposed pressure-pulse, or kinematic wave-based approach, combined with satellite-derived estimates of *ET* (to provide GR_p) will be useful in groundwater modeling applications for testing whether or not inclusion of the lag effect caused by the vadose zone is warranted or not.

It should be noted that the pixel size (1.1-km) may have a certain bearing on the results. With a smaller pixel size, one should expect only some changes of the shape and position of the modern and future period histogram of vadose zone lag times, shown in Fig. 11. However, the variability of D_{wt} within such pixels is smaller than the range of the vadose zone thickness (Fig. 5) as discussed in Section 3.1, which would result in nearly the same quantitative and qualitative conclusions.

5. Summary and conclusions

This study evaluates water movement through the vadose zone in areas within a large portion of the NSH (~44,600 km^2) where average *P* exceeds *ET* (over the 10-yr measurement period), leading to significant *GR*. Spatially distributed and high resolution (1.1-km) MODIS-based decade averaged $GR_{p,MODIS}$ rates for the modern period (2000–2009) provides the basis for calculating the pressure-based (or kinematic wave-based) velocities, which are then used to estimate vadose zone lag times. The analysis also relies on inputs of vadose zone thickness (depth to the water table), estimates of future period (2010–2099) GR_p rates from WRCP CMIP3 hydroclimate model projections, and estimates of hydraulic conductivity using the van Genuchten–Mualem equation. The proposed approach does not rely on parallel supercomputing, commonly involved in variably-saturated 3D numerical modeling of basin hydrology. Yet, it provides the desired high resolution, large scale (>10^5 km^2) simulation of soil moisture movement through the vadose zone under long-term average climate conditions.

This study answers four research questions with regard to the NSH: (1) What is the effect of a heterogeneous vadose zone thickness on the spatial distribution of vadose zone lag times? (2) How does soil hydraulic parameter uncertainty affect vertical velocity and vadose zone lag time estimates? (3) How are 21st century climate change projections expected to impact GR_p rates and vadose zone lag times? and (4) What is the percentage of surface area expected to experience changes in GR_a rates over time scales of 10, 50 and 100 years, typical of water planning and future climate modeling time scales? These questions are relevant for many other regions in the world and are needed for groundwater modeling applications, analysis of climate change impacts on groundwater, and the effective management and sustainability of future water resources.

In the NSH, the high spatial variability of vadose zone thickness and spatio-temporal variability of climatic conditions both influence the distribution and magnitude of the time lag between changes in deep drainage and actual *GR* at the water table. The mean vadose zone thickness is 21.9 m (σ = 15.6 m), while the mean GR_p rate and vadose zone lag time (τ) for the decade of 2000–2009 are 78 mm/yr and 5.28 yrs, respectively (for positive $GR_{p,\mathrm{MODIS}}$ pixels assuming baseline soil hydraulic parameters). Variability of *RSF*s was incorporated into the analysis of potential climate change effects through the selection of wet and dry hydroclimate scenarios from 112 GCM scenarios as nearest to $\pm 1\sigma$ from the mean *RSF* (1.21) for 2090–2099 in the NSH. Thus, the spatial mean GR_p rates for the future period are highly uncertain for the region and are projected to vary between a high of 212 mm/yr (*RSF* = 2.68) and a low of 47 mm/yr (*RSF* = 0.60), with end-of-century (2090–2099) *RSF*s of 1.63 and 0.76 for the wet and dry hydroclimate scenarios evaluated. The percentage of the NSH surface area expected to experience changes in GR_a rates (lag times calculated using $GR_{p,\mathrm{MODIS}}$ rates and baseline soil hydraulic parameters) is 89.9% in 10 yrs (2019), 99.6% in 50 yrs (2059), and 99.9% in 100 yrs (2099). The longest estimated future spatially averaged vadose zone lag time estimate in the NSH occurs when the GR_p from the dry scenario drops to a low of 47.2 mm/yr in the decade of 2030–2039, with a corresponding mean vadose zone lag time of 7.7 yrs. During that decade, ~75% of the NSH is expected to have lag times shorter than 10 yrs.

Hydraulic conductivity and vertical velocity (and thus, lag time) estimates in the NSH have uncertainties due to potential heterogeneity in geologic materials and limited data from field measurements. Sensitivity analyses reveal that saturated hydraulic conductivity is the most important hydraulic parameter, as expected, but that its sensitivity varies with moisture content and GR_p. Variations in vertical velocity and vadose zone lag time estimates due to uncertainty in K_s can be substantial. In fact, the expected range of possible K_s values leads to a greater change in estimated vadose zone lag times than do projected changes in end-of-century GR_p rates (2090–2099 relative to 2000–2009). The spatially averaged vadose zone lag time estimates range from 2.85 to 7.28 yrs for all K_s variations, and from 3.78 to 6.55 yrs for expected future climate variations (2090–2099). Therefore, it is quite clear that more detailed field characterization of hydrogeologic properties is desirable, especially when using hydrological models to make decisions about the future management of water resources impacted by climate change. These finding suggests that for the NSH, vadose zone model development efforts should be focused on assessment of model parameters, and they indicate that uncertainty caused by future GCM scenarios and downscaling methods are less important than those due to the hydrologic model, and not because a relatively simple model was used here.

While uncertainty in lag time estimates due to future climate projections and uncertainty in soil hydraulic parameters were explicitly evaluated, errors in lag time estimates associated with estimating D_{wt} and $GR_{p,\mathrm{MODIS}}$ rates, as well as assuming that long-term (10-yr) average GR_p rates can be used to accurately estimate long-term vertical velocities and lag times of soil moisture, can also be significant. As a caution, it should be stated that pressure heads and wetting fronts are not explicitly tracked with the simple gravity-driven kinematic velocity-based approach proposed here. That is why the approach should be used to estimate velocities and lag times under steady-state (~10-yr) climate conditions. Uncertainties arising from all of these factors combined preclude highly accurate prediction of lag time estimation even for regions with relatively homogeneous soil properties such as the NSH. Therefore, the proposed approach can only be used currently to obtain first-order estimates of the spatial distribution of lag times. At preliminary stages of work, these lag times indicate when the groundwater system will respond to changes in climate (as changes in diffuse GR_a). It is encouraging, however, that lag time estimates obtained here are consistent with those from previous field and more detailed modeling studies.

The proposed approach will be especially helpful in regions with longer vadose zone time lags than those of the NSH and more arid environments, where the water table is deeper and/or soil texture is finer. Additionally, many applications require shorter stress periods than analyzed here (decadal). So, this approach will be useful for testing whether or not inclusion of the lag effect caused by the vadose zone is warranted in groundwater modeling, with consideration of the desired temporal resolution. Overall, the proposed simple analytical approach to calculate gravity-driven vertical velocity provides a rapid quantitative screening tool that can be used to study lag times between changes in GR_p (deep drainage) and GR_a (at the water table) affected by spatially variable vadose zone thickness and climate change. The approach also provides estimates expected to have the same degree of uncertainty as those obtained from the use of advanced analytical and numerical solvers, such as the MODFLOW UZF1 Package, ParFlow, MikeShe, or HYDRUS, since their use also requires estimates of GR_p (or parameters to estimate actual *ET*) and soil hydraulic parameters. In summary, the proposed 1D vadose zone moisture modeling and GIS approach is applicable for use in semi-arid and arid regions with deep water tables and where long-term *P* and *ET* data for current and future conditions are available.

Acknowledgements

Funding was provided by the National Science Foundation IGERT program (DGE-0903469) to N. Rossman and V. Zlotnik, by the Agricultural Research Division of the University of Nebraska-Lincoln to J. Szilagyi, and by the ETH, Zurich, for a visiting professorship to V. Zlotnik. We acknowledge Kerry Hart (University of Nebraska-Lincoln) for helping with a Python script to process climate data, Tiejun Wang (University of Nebraska-Lincoln) for discussion of vadose zone hydrology in the NSH, one anonymous reviewer for constructive comments that helped improve the article, and the Program for Climate Model Diagnosis and Intercomparison (PCMDI) and the WCRP's Working Group on Coupled Modeling (WGCM) for their roles in making the WCRP CMIP3 multi-model dataset available. Support of this dataset is provided by the Office of Science, U.S. Department of Energy.

References

Allen, D.M., Cannon, A.J., Toews, M.W., Scibek, J., 2010. Variability in simulated recharge using different GCMs. Water Resour. Res. 46 (W00F03), 1–18.

Bleed, A.S., Flowerday, C.A. (Eds.), 1998. An Atlas of the Sand Hills, third ed. Conservation and Survey Division, University of Nebraska, Lincoln, NE.

Bouchet, R.J., 1963. Evapotranspiration reelle, evapotranspiration potentielle, et production agricole. Annal. Agronom. 14, 543–824.

Brekke, L., Thrasher, B.L., Maurer, E.P., Pruitt, T., 2013. Downscaled CMIP3 and CMIP5 climate projections: Release of downscaled CMIP5 climate projections, comparison with preceding information, and summary of user needs, 47 pp. <http://gdo-dcp.ucllnl.org/downscaled_cmip_projections/techmemo/downscaled_climate.pdf> (accessed December 2013).

Brunner, P., Doherty, J., Simmons, C.T., 2012. Uncertainty assessment and implications for data acquisition in support of integrated hydrologic models. Water Resour. Res. 48 (W07513), 1–18.

Carsel, R.F., Parrish, R.S., 1988. Developing joint probability distributions of soil water retention characteristics. Water Resour. Res. 24, 755–769.

Chen, X., Chen, X., 2004. Simulating the effects of reduced precipitation on ground water and streamflow in the Nebraska Sand Hills. J. Am. Water Resour. Assoc. 40 (2), 419–430.

Chen, X., Chen, X., Rowe, C., Hu, Q., Anderson, M., 2003. Geological and climatic controls on streamflows in the Nebraska Sand Hills. J. Am. Water Resour. Assoc. 39 (1), 217–228.

Cook, P.G., Jolly, I.D., Walker, G.R., Robinson, N.I., 2003. From drainage to recharge to discharge: some timelags in subsurface hydrology. In: Alsharhan, A.S., Wood, W.W. (Eds.), Water Resources Perspectives: Evaluation, Management and Policy. Elsevier BV, Amsterdam, The Netherlands, pp. 319–326.

Crosbie, R.S., McCallum, J.L., Walker, G.R., Chiew, F.H.S., 2010. Modelling climate-change impacts on groundwater recharge in the Murray-Darling Basi0, Australia n. Hydrogeol. J. 18 (7), 1639–1656.

Crosbie, R.S., Dawes, W.R., Charles, S.P., Mpelasoka, F.S., Aryal, S., Barron, O., Summerell, G.K., 2011. Differences in future recharge estimates due to GCMs, downscaling methods and hydrological models. Geophys. Res. Lett. 38 (L11406), 1–5.

Crosbie, R.S., Scanlon, B.R., Mpelasoka, F.S., Reedy, R.C., Gates, J.B., Zhang, L., 2013. Potential climate change effects on groundwater recharge in the High Plains aquifer, USA. Water Resour. Res. 49 (7), 3936–3951.

Ferguson, I.M., Maxwell, R.M., 2012. Human impacts on terrestrial hydrology: climate change versus pumping and irrigation. Environ. Res. Lett. 7 (044022), 1–8.

Gosselin, D.C., Rundquist, D.C., McFeeters, S.K., 2000. Remote monitoring of selected ground-water dominated lakes in the Nebraska Sand Hills. J. Am. Water Resour. Assoc. 36 (5), 1039–1051.

Graham, D.N., Butts, M.B., 2005. Flexible integrated watershed modeling with MIKE SHE, in: Singh, V.P., Frevert, D.K. (Eds.), Watershed Models. CRC Press, Boca Raton, FL, USA, pp. 245–272. <http://mikebydhi-cn.com/upload/dhisoftwarearchive/papersanddocs/waterresources/MSHE_Book_Chapter/MIKE_SHE_Chp10_in_VPSinghDKFrevert.pdf> (accessed August 2013).

Green, T.R., Taniguchi, M., Kooi, H., Gurdak, J.J., Allen, D.M., Hiscock, K.M., Treidel, H., Aureli, A., 2011. Beneath the surface of global change: impacts of climate change on groundwater. J. Hydrol. 405 (3–4), 532–560.

Grismer, M.E., 2013. Estimating agricultural deep drainage lag times to groundwater: application to Antelope Valley, California, USA. Hydrol. Process. 27, 378–393.

Gurdak, J.J., Hanson, R.T., McMahon, P.B., Bruce, B.W., McCray, J.E., Thyne, G.D., Reedy, R.C., 2007. Climate variability controls on unsaturated water and chemical movement, High Plains aquifer, USA. Vadose Zone J. 6 (2), 533–547.

Harvey, F.E., Swinehart, J.B., Kurtz, T.M., 2007. Ground water sustenance of Nebraska's unique Sand Hills peatland fen ecosystems. Ground Water 45 (2), 218–234.

Healy, R.W., 2010. Estimating Groundwater Recharge. Cambridge University Press.

Hill, M.C., 2006. The practical use of simplicity in developing ground water models. Ground Water 44 (6), 775–781.

Holmes, K.W., Chadwick, O.A., Kyriakidis, P.C., 2000. Error in a USGS 30-meter digital elevation model and its impact on terrain modeling. J. Hydrol. 233 (1–4), 154–173.

IPCC, 2000. Nakicenovic N., Swart, R. (Eds.), Emissions scenarios: Special report. Cambridge University Press.

Istanbulluoglu, E., Wang, T., Wright, O.M., Lenters, J.D., 2012. Interpretation of hydrologic trends from a water balance perspective: the role of groundwater storage in the Budyko hypothesis. Water Resour. Res. 48 (W00H16), 1–22.

Knutti, R., Masson, D., Gettelman, A., 2013. Climate model genealogy: generation CMIP5 and how we got there. Geophys. Res. Lett. 40 (6), 1194–1199.

Kollet, S.J., Maxwell, R.M., 2008. Capturing the influence of groundwater dynamics on land surface processes using an integrated, distributed watershed model. Water Resour. Res. 44 (W02402), 1–18.

Kollet, S.J., Maxwell, R.M., Woodward, C.S., Smith, S., Vanderborght, J., Vereecken, H., Simmer, C., 2010. Proof of concept of regional scale hydrologic simulations at hydrologic resolution utilizing massively parallel computer resources. Water Resour. Res. 46 (W04201), 1–7.

Liang, X., Lettenmaier, D.P., Wood, E.F., Burges, S.J., 1994. A simple hydrologically based model of land surface water and energy fluxes for general circulation models. J. Geophys. Res.–Atmos. 99 (D7), 14415–14428.

Loope, D.B., Swinehart, J.B., 2000. Thinking like a dune field: geological history in the Nebraska Sand Hills. Gt. Plains Res. 10 (1), 5–35.

Loope, D.B., Swinehart, J.B., Mason, J.P., 1995. Dune-dammed paleovalleys of the Nebraska Sand Hills: intrinsic versus climatic controls on the accumulation of lake and marsh sediments. Geol. Soc. Am. Bull. 107 (4), 396–406.

Mason, J.A., Swinehart, J.B., Goble, R.J., Loope, D.B., 2004. Late-Holocene dune activity linked to hydrological drought, Nebraska Sand Hills, USA. The Holocene 14 (2), 209–217.

McGuire, V.L., 2011. Water-level changes in the High Plains aquifer, predevelopment to 2009, 2007–08, and 2008–09 and change in water in storage, predevelopment to 2009. U.S. Geol. Surv. Sci. Invest. Rep. 2011–5089, 13 pp.

McMahon, P.B., Dennehy, K.F., Michel, R.L., Sophocleous, M.A., Hurlburt, D.B., 2003. Water movement through thick unsaturated zones overlying the Central High Plains aquifer, southwestern Kansas, 2000–2001. U.S. Geol. Surv. Water-Resour. Invest. Rep. 03-4171, 32 pp.

McMahon, P.B., Dennehy, K.F., Bruce, B.W., Bohlke, J.K., Michel, R.L., Gurdak, J.J., Hurlburt, D.B., 2006. Storage and transit time of chemicals in thick unsaturated zones under rangeland and irrigated cropland, High Plains, United States. Water Resour. Res. 42 (W03413), 1–18.

Morton, F.I., Ricard, F., Fogarasi, F., 1985. Operational estimates of areal evapotranspiration and lake evaporation—program WREVAP. National Hydrologic Research Institute Paper #24. Ottawa, Canada.

Mualem, Y., 1976. A new model predicting the hydraulic conductivity of unsaturated porous media. Water Resour. Res. 12 (3), 513–522.

Munch, Z., Conrad, J.E., Gibson, L.A., Palmer, A.R., Hughes, D., 2013. Satellite earth observation as a tool to conceptualize hydrogeological fluxes in the Sandveld, South Africa. Hydrogeol. J. 21 (5), 1053–1070.

Niswonger, R., Prudic, D.E., Regan, R.S., 2006. Documentation of the Unsaturated-Zone Flow (UZF1) Package for modeling unsaturated flow between the land surface and the water table with MODFLOW-2005. U.S. Geol. Surv. Tech. Meth. 6-A19, 62 pp.

NRCS (Natural Resources Conservation Service), 2006. U.S. General Soil Map (STATSGO2). Natural Resources Conservation Service, United States Department of Agriculture. <http://soildatamart.nrcs.usda.gov/> (accessed August 2013).

Ong, J.T., 2010. Investigation of spatial and temporal processes of lake-aquifer interactions in the Nebraska Sand Hills. Ph.D. dissertation, University of Nebraska-Lincoln. <http://digitalcommons.unl.edu/geoscidiss/13/> (accessed October 2012).

Peterson, S.M., Stanton, J.S., Saunders, A.T., Bradley, J.R., 2008. Simulation of ground-water flow and effects of ground-water irrigation on base flow in the Elkhorn and Loup River Basins, Nebraska. U.S. Geol. Surv. Sci. Invest. Rep. 2008-5143, 65 pp.

Philip, J.R., 1957. The theory of infiltration: 2. The profile of infinity. Soil Sci. 83 (6), 435–448.

Priestley, C.H.B., Taylor, R.J., 1972. On the assessment of surface heat flux and evaporation using large-scale parameters. Monthly Weather Rev. 100, 81–92.

PRISM (Parameter-elevation Regressions on Independent Slopes Model) Climate Group, 2012. Oregon State University Climate Data. <http://prism.oregonstate.edu> (accessed October 2012).

Rasmussen, T.C., 2001. Pressure wave vs. tracer velocities through unsaturated fractured rock. In: Evans, D.D., Nicholson, T.J., Rasmussen, T.C. (Eds.), Flow and Transport through Unsaturated Fractured Rock. American Geophysical Union, Washington, DC, pp. 45–52.

Rossman, N.R., Zlotnik, V.A., 2013. Review: regional groundwater flow modeling in heavily irrigated basins of selected states in the western United States. Hydrogeol. J. 21 (6), 1173–1192.

Rundquist, D.C., 1983. Wetland inventories of Nebraska's Sandhills. Resource report, Publication 9, Conservation and Survey Division, University of Nebraska, Lincoln, NE.

Scanlon, B.R., Keese, K.E., Flint, A.L., Flint, L.E., Gaye, C.B., Edmunds, W.M., Simmers, I., 2006. Global synthesis of groundwater recharge in semiarid and arid regions. Hydrol. Process. 20 (15), 3335–3370.

Scanlon, B.R., Reedy, R.C., Tachovsky, J.A., 2007. Semiarid unsaturated zone chloride profiles: archives of past land use change impacts on water resources in the southern High Plains, United States. Water Resour. Res. 43 (W06423), 1–13.

Scanlon, B.R., Reedy, R.C., Gates, J.B., Gowda, P.H., 2010. Impact of agroecosystems on groundwater resources in the Central High Plains, USA. Agric. Ecosyst. Environ. 139 (4), 700–713.

Schewe, J., Heinke, J., Gerten, D., Haddeland, I., Arnell, N.W., Clark, D.B., Dankers, R., Eisner, S., Fekete, B.M., Colon-Gonzalez, F.J., Gosling, S.N., Kim, H., Liu, X., Masaki, Y., Portmann, F.T., Satoh, Y., Stacke, T., Tang, Q., Wada, Y., Wisser, D., Albrecht, T., Frieler, K., Piontek, F., Warszawski, L., Kabat, P., 2013. Multimodel assessment of water scarcity under climate change. Proc. Natl. Acad. Sci. 111 (9), 1–6.

Schmieder, J., Fritz, S.C., Swinehart, J.B., Shinneman, A.L.C., Wolfe, A.P., Miller, G., Daniels, N., Jacobs, K.C., Grimm, E.C., 2011. A regional-scale climate reconstruction of the last 4000 years from lakes in the Nebraska Sand Hills, USA. Quat. Sci. Rev. 30 (13–14), 1797–1812.

Schwartz, M.O., 2006. Numerical modelling of groundwater vulnerability: the example Namibia. Environ. Geol. 50 (2), 237–249.

Sisson, J.B., Ferguson, A.H., van Genuchten, M.Th., 1980. Simple method for predicting drainage from field plots. Soil Sci. Soc. Am. J. 44 (6), 1147–1152.

Smith, R.E., 1983. Approximate soil water movement by kinematic characteristics. Soil Sci. Soc. Am. J. 47 (1), 3–8.

Sousa, M.R., Jones, J.P., Frind, E.O., Rudolph, D.L., 2013. A simple method to assess unsaturated zone time lag in the lag time from ground surface to receptor. J. Contam. Hydrol. 144 (1), 138–151.

Soylu, E., Istanbulluoglu, E., Lenters, J.D., Wang, T., 2010. Quantifying the impact of groundwater depth on evapotranspiration in a semi-arid grassland region. Hydrol. Earth Syst. Sci. 7, 6887–6923.

Stephens, D.B., 1995. Vadose Zone Hydrology. CRC Press.

Strassberg, G., Scanlon, B.R., Chambers, D., 2009. Evaluation of groundwater storage monitoring with the GRACE satellite: case study of the High Plains aquifer, central United States. Water Res. Res. 45 (W05410), 1–10.

Summerside, S., Ponte, M., Dreeszen, V.H., Hartung, S.L., Khisty, M.J., Szilagyi, J., 2001. Update and Revision of Regional 1×2 degree Water-table Configuration Maps for the State of Nebraska. Conservation and Survey Division, University of Nebraska, Lincoln, NE.

Sweeney, M.R., Loope, D.B., 2001. Holocene dune-sourced alluvial fans in the Nebraska Sand Hills. Geomorphology 38 (1–2), 31–46.

Szilagyi, J., Jozsa, J., 2013. MODIS-aided statewide net groundwater-recharge estimation in Nebraska. Ground Water 51 (5), 735–744.

Szilagyi, J., Harvey, F.E., Ayers, J.F., 2003. Regional estimation of base recharge to ground water using water balance and a base-flow index. Ground Water 41 (4), 504–513.

Szilagyi, J., Jozsa, J., Kovacs, A., 2011a. A calibration-free evapotranspiration mapping (CREMAP) technique. In: Labedzki, L. (Ed.), Evapotranspiration. InTech, Rijeka, Croatia, pp. 257–274.

Szilagyi, J., Zlotnik, V.A., Gates, J., Jozsa, J., 2011b. Mapping mean annual groundwater recharge in the Nebraska Sand Hills, USA. Hydrogeol. J. 19 (8), 1503–1513.

Szilagyi, J., Zlotnik, V.A., Jozsa, J., 2013. Net recharge vs. depth to groundwater relationship in the Platte River Valley of Nebraska, United States. Ground Water 51 (6), 945–951.

Toews, M.W., Allen, D.M., 2009. Evaluating different GCMs for predicting spatial recharge in an irrigated arid region. J. Hydrol. 374 (3–4), 265–281.

USBR (U.S. Bureau of Reclamation), 2010. Climate change and hydrology scenarios for Oklahoma yield studies. Technical Memo. 86-68210-2010-01, 59 pp. <http://www.meted.ucar.edu/USBR/water_climate/media/graphics/Reclamation2010_OTAO_Report_Final-100402.pdf> (accessed June 2013).

USBR (U.S. Bureau of Reclamation), 2011. West-wide climate risk assessments: Bias-corrected and spatially downscaled surface water projections. Technical Memo. 86-68210-2011-01, 138 pp. <http://www.usbr.gov/WaterSMART/docs/west-wide-climate-risk-assessments.pdf> (accessed May 2013).

USGS (U.S. Geological Survey), 1999. Nebraska Elevation Data, National Elevation Dataset, 7.5-minute. U.S. Geol. Surv., EROS Data Center, Sioux Falls, SD. <http://snr.unl.edu/data/geographygis/elevation/NEDSDownload.asp> (accessed June 2012).

USGS (U.S. Geological Survey), 2010. National Hydrography Dataset. U.S. Geol. Surv. <http://dnr.ne.gov/databank/nhd.html> (accessed June 2012).

van Genuchten, M.Th., 1980. A closed-form equation for predicting the hydraulic conductivity of unsaturated soils. Soil Sci. Soc. Am. J. 44 (5), 892–898.

Wang, T., Istanbulluoglu, E., Lenters, J., Scott, D., 2009. On the role of groundwater and soil texture in the regional water balance: an investigation of the Nebraska Sand Hills, USA. Water Resour. Res. 45 (W10413), 1–13.

Warrick, A.W., Biggar, J.W., Nielson, D.R., 1971. Simultaneous solute and water transfer for an unsaturated soil. Water Resour. Res. 7 (5), 1216–1225.

Wilson, J.L., 1974. Dispersive mixing in a partially saturated porous medium. Ph.D. dissertation, Massachusetts Institute of Technology. <http://dspace.mit.edu/handle/1721.1/13844> (accessed July 2013).

Wilson, J.L., Gelhar, L.W., 1981. Analysis of longitudinal dispersion in unsaturated flow 1. The analytical method. Water Resour. Res. 17 (1), 122–130.

Zlotnik, V.A., Burbach, M., Swinehart, J., Bennett, D., Fritz, S., Loope, D.B., Olaguera, F., 2007. Using direct-push methods for characterization in dune-lake environments of the Nebraska Sand Hills. Environ. Eng. Geosci. 8 (3), 205–216.

Zlotnik, V.A., Robinson, N.I., Simmons, C.T., 2010. Salinity dynamics of discharge lakes in dune environments: conceptual model. Water Resour. Res. 46 (W11548), 1–10.